Carbonate apatite formulation in cuticle structure adds resistance to microbial attack for American lobster

JOSEPH G. KUNKEL[1*] & MICHAEL J. JERCINOVIC[2]

[1]Biology Department, University of Massachusetts, Amherst, MA, USA, and **[2]**Geosciences Department, University of Massachusetts, Amherst, MA, USA
*Correspondence: Joseph G. Kunkel, Center for Land Sea Interaction, Marine Science Center, University of New England, Biddeford ME 04005, USA. E-mail: joe@bio.umass.edu

Abstract

Various carbonate apatite formulae contribute to discrete cuticle structures participating in protective functions of the American lobster, *Homarus americanus*, integument. Canal walls use their lowest Calcium : Phosphate (Ca:P) ratios to protect exposed surfaces of gland and neuronal canals. The linings insulate more soluble calcium carbonate from attack by acid secreting micro-organisms. A trabecular bone-like structure, called here 'trabeculae' in analogy to vertebrates, utilizes high Ca:P in the inner exocuticle demonstrating an efficient use of environmentally scarce phosphate and provides the hardness layer of the cuticle that protects the superficial calcite layer from flexure. Strength is derived from phosphatic trabeculae being embedded in a phenolicly hardened inner exocuticle layer. A third location and use of carbonate apatite is at the interface of the calcite and inner exocuticle where it may cap calcite layer development. A fourth phosphatic localization is seen in cuticular nipples that accompany the site of organule canal entry at the epidermal face of the cuticle. This high Ca:P localization may be associated with accumulation of Ca and P by canal forming cells for use in the nascent canal wall construction. A schematic model of the cuticle emphasizes regional diversity of a composite cuticle suggesting mineral function. An outer calcite crystalline layer provides a dense barrier that dissolves slowly through an intact epicuticle providing an external alkaline unstirred layer inhibitory to bacterial physiology. Superficial injury to the epicuticle and calcite layer provides a stronger flush of alkalinity from bared calcite or deeper rapidly dissolving amorphous calcium carbonate, generating a concerted general immune response by increasing alkalinity of the unstirred layer.

Key words: *Carbonate apatite, calcite, unstirred layer, antimicrobial pH*

Introduction

The mineralization of cuticle in the American lobster, *Homarus americanus* H. Milne Edwards, 1837, is reportedly dominated by calcite and amorphous calcium carbonate (Lowenstam 1981; Raabe et al. 2005). These compounds are the most abundant minerals in the ocean environment. They comprise the major building materials for most shellfish along with aragonite, another crystalline form of calcium carbonate. The utilization of phosphate compounds as a crustacean skeletal building material is considered archaic (Vega et al. 2005; Buckeridge & Newman 2006), i.e. found in extinct forms when phosphate was less limiting but more rarely in current shellfish. Indeed, phosphate itself is a growth-limiting resource in many current marine environments. Phosphate has been considered to occur mainly in its amorphous form in lobster cuticle and is only transformed to crystalline apatite by high-temperature treatment (Al-Sawalmih et al. 2009).

A phosphate compound, a carbonate apatite, is used in construction of barnacle shell plates of particular species of the genus *Ibla* (Lowenstam & Weiner 1992), but has not been found in other barnacle species or in decapods in general. In constructing a model of lobster cuticle ab initio from a base of average composition, phosphatic contributions have been ignored (Nikolov et al. 2011). However, we have found evidence using high-resolution X-ray backscatter that discretely different compounding formulae of carbonate apatite are used in a very focused way in the American lobster to achieve cuticle properties not achievable using calcium carbonate alone (Kunkel et al.

2012). Here we more fully document four ways that carbonate apatite is used in constructing the cuticle of the American lobster that are significant, directly and indirectly, in the cuticle's role of insulating the lobster from its environment.

Materials and methods

Animals

American lobster adults were obtained from several sources, all in the New England USA coastal area. Undersized (shell disease symptomless) control lobsters (<83 mm carapace length, CL) were obtained from the Maine Ventless Trap Program courtesy of Carl Wilson, Maine DMR, from an area between Isle of Shoals NH and Kennebunk ME. CL is defined as the distance measured by callipers from the lobster carapace eye-notch to the intersection of the carapace dorsal suture with the hind edge of the carapace. Large control (shell disease symptomless) lobsters (>83 mm CL) and shell diseased lobsters were obtained from Thomas Angell of the RI University SeaGrant Program from Naragansett Bay, RI. Impoundment shell diseased lobsters were provided from the Bigelow Aquarium, Boothbay Harbor, Maine. One early shell diseased lobster was obtained via trawling by the NOAA Ship Albatross IV from a deep-water canyon on the edge of the continental shelf directly south of Narragansett Bay, RI. The Maine control lobsters were kept at 15ºC in a natural seawater gravity-fed life table in the Marine Sciences Center at University of New England, Biddiford, Maine during July and August or transferred to a recirculating marine tank at 15ºC in Amherst, MA, September-June. Lobsters were fed ad lib scallop meats on a daily basis.

Tissue preparation

Pieces of cuticle approximately 1 cm square were cut from the dorsal carapace and plunge-frozen in liquid nitrogen-cooled propane and subsequently transferred to liquid nitrogen-cooled acetone to dehydrate as they warmed to room temperature over a 24-h period. The large format allowed searching for the canal structures, which are separated on average by 700 μm.

The dehydrated cuticle was embedded in EpoThin epoxy resin in 25-mm blocks and prepared for viewing in the electron microprobe (EMP) by grinding with carborundum paper and polishing with graded diamond (6, 3, 1, 0.25 μm) suffused lapping cloths (Metadi) until the desired polished surface was achieved.

Macro images of raw and polished cuticle were taken with a high resolution digital camera (DuncanTech DT4000) mounted of a zoom scope (Applicable Electronics). EMP raster compositional images of polished cuticle were taken with a *Cameca* SX-100 EMP with a limiting resolution of 1/3 μm. Line transects of composition of cuticle were obtained with a *Cameca* SX-50 EMP.

Compositional EMP data were analyzed with *ad hoc* written R-scripts which provide computational directions in
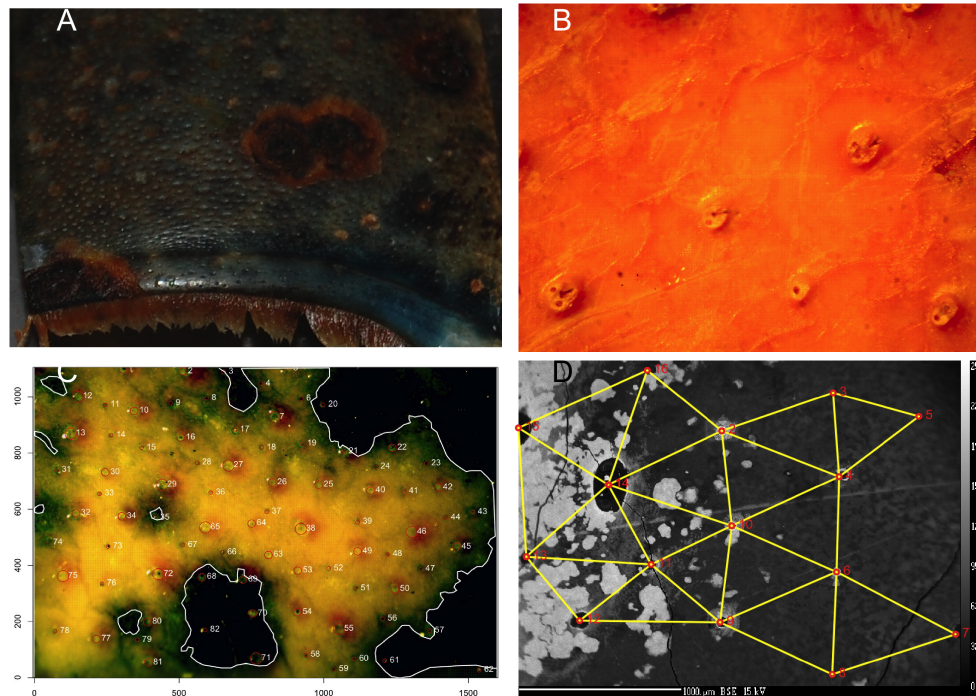

Figure 1. Organule structures in the lobster cuticle. A. Carapace sector of cuticle, posterior right of the median. Three mature shell disease lesions are marked by large asterisks. A smaller asterisk separates two smaller lesions. Dimples in the cuticle are locations of over-dispersed organules. B. Higher-resolution view of cuticle cleaned and fixed in alcohol showing several organules, three are marked 13, which refer to sequential stages in organule development. C. High-resolution image at a broader perspective where four size stages of organule can be discerned. D. An EMP backscatter image of a tangentally polished carapace cuticle in which 15 organule foci are identified and their distances to neighbors measured.

the R computational environment, the Gnu-Public (free) software we use for all our data analysis (R Development Core Team 2011). The custom R-scripts are available with data exemplars from the first author by email request.

Results

Cuticle structural heterogeneity

The cuticle of lobsters uses carbonate apatite in four relatively discrete situations, two of which have immediate rational structural functions and a second two whose function are more debatable. The first identified role is the use of apatite and various formulae of carbonate apatite to line gland and neural canals through the lobster cuticle. The lobster cuticle surface is covered with organules (Fig 1A,B), are discrete structures (Merritt 2007) which are either glands or sensory organules. They tend to be overdisperse as seen by their arrangement in hexagonal pattern (Fig 1C,D) and in the particular instance of Fig 1D, the strut distance from one organule to another is 690 ±110 μm standard deviation, which is typical, but the exact range varies depending on the expansion experienced at the last moult. This provides substantial inter-organule space occupied by pavement-type epidermal cells that produce the typical cuticle layers of the lobster integument. Both canal types, gland and neurite, use carbonate apatite as a canal lining through which either the dermal glands secrete substance onto the cuticle surface or in which sensory neurons send neurites through the protective canal to innervate a cuticle surface sensory bristle. These sensory and glandular organules may be combined together to form composite organules with multiple canals serving either secretion, neurite conduction or combinations of the two functions. The multiple canal organules most likely develop over a sequence of moults in which a new gland organule is established new at one moult and accrues a bristle canal or another gland canal during subsequent moults.

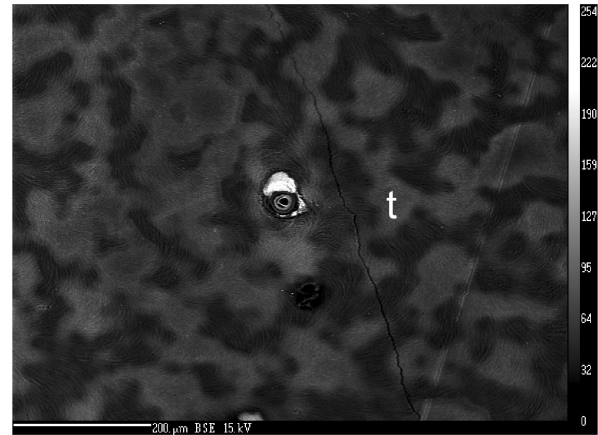Organules are in size classes that suggest at least three to

Figure 2. Lobster carapace cuticle tangentally polished down into the inner exocuticle, showing an organule canal with a surrounding collar of calcite that provides the highest electron backscatter intensity. The surrounding field has phosphate-rich trabeculae, identified in the image with a relatively high backscatter intensity compare to the phosphate-poor intervening areas.

four stages of development (Fig 1B,C). In growth during the moulting process the lobster cuticle expands approximately 10% in linear dimensions, which translates to a 21% increase in cuticle area at each moult. The density of organules is maintained from instar to instar, which thus requires generation and insertion of approximately one new organule per five pre-existing organules as described by Lawrence (1966) for insect integument.

Second, the inner exocuticle of lobsters utilizes an organization of carbonate apatite which is here termed 'trabeculae', in structural analogy to the vertebrate trabecular bone, to create a rigid structure that represents the hardness of the lobster cuticle (Fig 2 in tangential and Fig 3 in transverse cross-section). The hardness profile of lobster cuticle has been measured (Raabe et al. 2005), demonstrating a thin soft outer exocuticle, which we show
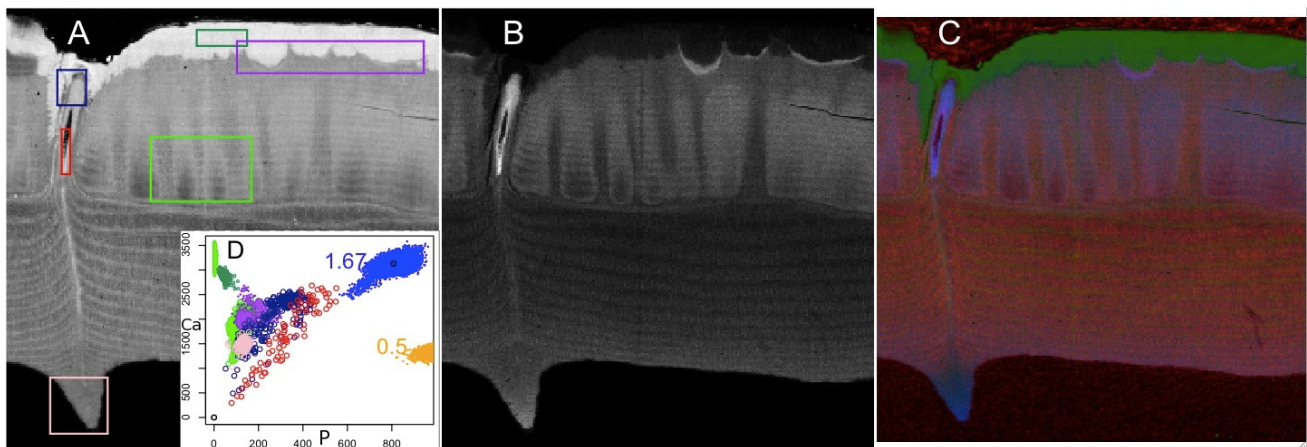

Figure 3. Lobster carapace cuticle transversely polished and analysed for Compositional EMP of Ca, P and Cl. A. Ca X-ray backscatter image with boxes indicating areas that were focused on with singular-value decomposition to identify calcium and phosphate areas with identifiable Ca : P ratios. B. P X-ray backscatter image. C. False colour presentation of Ca (green), P (blue) and Cl (red) map of lobster cuticle. D. Pixel Ca vs. P molar proportional content derived from panels A and B delimited areas. The pixels for plotting were chosen by a principal component function that identified the calcite pixels (dark green sector) or phosphatic sectors (all other colours).

to be the calcite layer. The hardest layer is the inner exocuticle and the softest layer is the endocuticle. We show that the major difference between the inner exocuticle and the endocuticle is the trabeculae of the inner exocuticle.

A third, less-prominent, carbonate apatite structure is observed often at the interface of the calcite and inner exocuticle (Fig 3B,C). This phosphatic structure based on its location may be associated with the inner-capping of crystallization of the calcite layer.

A fourth regularly observed structure is found associated in a cone of inward-projecting endocuticle membranous layer (Fig 3C), which occurs where the canals of organules exit the inner face of the nascent cuticle to interface with gland cells and neurons. All of these structures have limited spatial extent and are dominated by their being embedded in a background of more pervasive calcite and amorphous calcium carbonate, because of which they have been missed or ignored in the past.
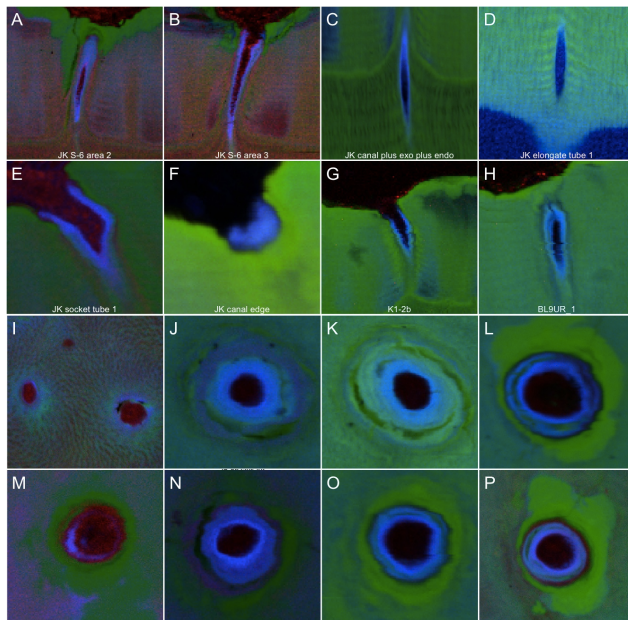

Figure 4. Lobster carapace organule canal sections as EMP determined mineral content displayed in false colour images with Ca as green, P as blue and another atom type (Cl, F, or K) displayed as red. A#H. Transversely polished cuticle faces. I#P. Tangentially polished cuticle faces. A,B,G,H third atom is K which marks surface microorganism internal potassium. All other red colouring is for Cl content.

Cuticle chemical heterogeneity

The experimental basis of the assertion that observed phosphatic structures are carbonate apatite depends upon Compositional EMP, which allows the identity and amount of atomic elements to be established for raster images of polished surfaces at a less than micron resolution. By collecting pixel-wise K-alpha spectra for multiple atomic elements one can determine the relative amounts of each element at each pixel location. The structures involved are on the order of microns or more in thickness and are well-resolved by the images obtained with the *Cameca* SX-100

EMP.Epoxy resin-embedded lobster cuticle fragments were polished either as transects perpendicular to the surface or as tangential sections parallel to the surface of the cuticle. This allowed the mineral signatures to be viewed in two perspectives that added three-dimensional perspective on their structure. Fig 3 illustrates a sample in which three elements were analysed, Ca, P in Figs 3A and 3B, and chloride (Cl) (Cl map not shown). In Fig 3C they are combined into a false colour image by assigning blue to P, green to Ca and red to Cl. This protocol allowed other samples to be easily categorized and further analyzed. In Fig 3D the molar Ca and P content of pixels are plotted from particular colour delimited zones in Fig 3A. The pixels were chosen for plotting according to a principal components function applied to the delimited data that allowed calcite type pixels or carbonate apatite type pixels to be chosen. Using this pixel-selection approach for the light violet zone in Fig 3A only the phosphatic cap-pixel's Ca and P contents are plotted in Figure 3D. This illustrates the variety of Ca:P ratios used in focal structures of the cuticle. Indeed, two ratios of Ca:P consistent with carbonate apatite formulations are used in the canal section as seen by the red and dark blue marked Ca:P ratios in Fig 3D.

Figs 4A-P illustrate a collection of longitudinally sectioned (A-H) and tangentially sectioned (I-P) canals in false colour, allowing the character of the mineral structures to be identified visually in one image. Using these types of images and analyses similar to Fig 3D, the Ca:P ratio and depth of the structure in the cuticle were judged. Depth in the cuticle was based on its association with the surface calcite layer or other surrounding structural environments such as the presence of calcite intrusions or phosphatic trabeculae. When the canal cross-section was surrounded by calcite it was given a nominal 0.1 depth designation. When a canal had a section of calcite collar on one side as seen in Figs 2A and 3A it was given a nominal 0.2 depth designation. When a canal transect was surrounded by trabeculae but no calcite collar it was assigned a 0.5 depth. If a canal was at the exocuticle-endocuticle interface it was assigned a 1.0 depth. If a canal had no trabeculae surrounding it and relatively less-dense endocuticle lamellae it was considered to be in the endocuticle region and given a 1.5 depth designation. The resultant cross-section data are thus grouped into reasonably defined depth regions of the cuticle based on visual landmarks. In tangentially polished cuticle the slight curvature of the cuticle provides areas that transition smoothly through all the cuticle levels and the approximate depth of a canal can be estimated by interpolating the distance between the three reference levels: epicuticle surface (0.0), exo/endocuticle ecdysial line (1.0), cuticle#epidermal boundary (2.0) using macroimages such as Fig 1D to assign the depth. Figs 4A-H are a collection of canal transects catching the canal in approximate longitudinal section at various depths below the surface of the cuticle. The average depth of the structure was again assigned by recording the mid-depth of the structure using the epicuticle surface as level 0, the exo- and
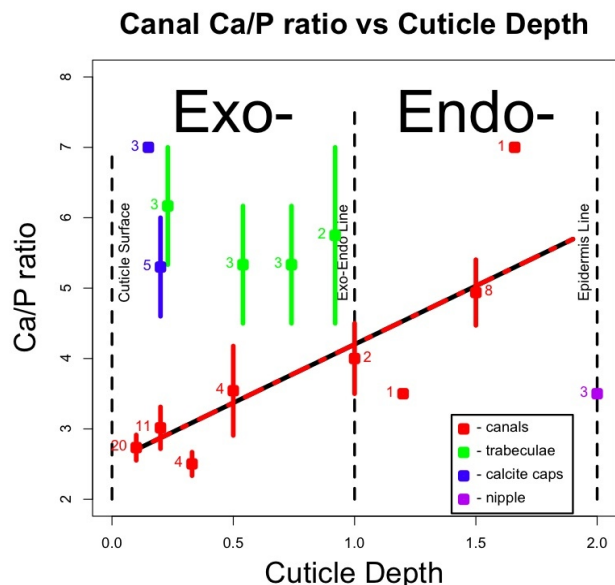
Canal Ca/P ratio vs Cuticle Depth

Figure 5. Structural Ca : P ratios for the four distinct uses of P in lobster carapace cuticle. The depth categories of the structures were assigned by circumstantial rules and averages were created within those categories.

endocuticle ecdysial line separating as 1.0 and the epidermal border as 2.0.

If the ratio of Ca:P derived from the structures exemplified in Figs 4A-P is plotted against their estimated depth in the cuticle it is seen that the lowest Ca:P ratios occur close to the cuticle surface (Fig 5). A few canals actually exhibited the Ca:P ratio of apatite, i.e. 1.667, which has no carbonate in its formula. Non-carbonate apatite itself is the most resistant of the apatites to acid, thus the canal linings closest to the seawater environment are the most resistant to potential sources of environmental acid.

Discussion

The description of the mineral heterogeneity of lobster cuticle (Kunkel et al. 2012) using high-resolution X-ray backscatter needs further elaboration to relate its heterogeneous formulae to its several roles in the cuticle for insulating the animal from environmental attacks. Here we focus on the variety of carbonate apatites and propose more explicitly the properties and functions for them in lobster cuticle. First, carbonate apatite has never been identified as a significant part of the native structure of lobster cuticle and thus its potential in providing any benefit to the lobster integument has not been considered seriously. Previous looks at lobster cuticle mineral content have used X-ray diffraction on ground-up whole cuticle using the X-ray powder diffraction pattern to identify apatite that is seen as a minor peak in sintered samples but is not seen in native samples (Romano et al. 2007).

Sintering converts diverse crystalline forms of carbonate apatite and amorphous calcium phosphate to apatite by driving off carbonate as carbon dioxide. Several formulations of carbonate apatite are observed with the

EMP Electron Micro Probe in discrete structures in natural cuticle. The sintered cuticle does not provide strong signals for any particular apatite and thus apatites have been overlooked as significant components in lobster cuticle. The limited apatite profiles in powder pattern quantitative analysis depends upon the fact that the most highly phosphatic structures, the gland and neurite canals, are sparse from a cross-sectional point of view. Second, the wider use of phosphate in the carbonate apatite trabeculae is restricted to the inner exocuticle and has the lowest P content of available bone formulae. The use of the high Ca:P carbonate apatite formulation in lobster trabeculae is consistent with the need to be very sparing in the use of environmentally sparse phosphate and furthermore saving phosphate for more essential needs such as membrane phospholipids, phosphoproteins, DNA and RNA synthesis.

We use the term 'cuticle trabeculae' for the lobster cuticle phosphatic structures limited to the inner exocuticle in its structural meaning. 'Trabeculae' in morphological terminology refers to struts of material and has been used as 'trabeculae carneae' to describe particular heart muscle morphology (Pérez et al. 2008) and 'splenic trabeculae' used to describe vertebrate spleen tissue structure (Kühnel 2003). We propose the term 'cuticle trabeculae' to describe the carbonate apatite struts that we propose strengthen the inner exocuticle and provide a rigid platform on which to hold the crystalline calcite layer which in our model, Fig 6, is the primary impervious layer to microbial attack. First, the calcite forms a close to solid crystalline structure, seen in Figures 1D and 3A, that would physically prevent microbes from reaching organic substrate to digest. Second, the slow dissolution of the calcite through the epicuticular layer into the thin unstirred layer (Pohl et al. 1998) adjusts its pH toward the pK of calcite, pH 9.0 (Kunkel et al. 2012).

Thus, while dissolution of CO_2 into seawater tends to lower the pH, the inherent calcite, aragonite and amorphous calcium carbonate of shell structures of shellfish dissolving tends to increase the pH in the unstirred layers surrounding those shells. The cuticle trabeculae underlying the lobster calcite layer, as drawn in Fig 6, prevent the calcite layer from bending and flexing that would lead to cracks and entry points for microbial attack.

The presence of a phosphate adjacent to the inner surface of the calcite layer is consistent with a capping of the calcite layer via phosphate poisoning of crystal growth (Simkiss 1964). The calcite inner exocuticle boundary represents where the pore filaments from the epidermal cells terminate. The secretion of calcium phosphate at the pore filament termini is a logical mechanism by which the thickness of the calcite layer could be dynamically controlled as part of the living space of the lobster cuticle.

The crystallization process of the calcite layer excludes the pore filaments which retreat from the calcite layer, but the secretion of phosphate by the pore filaments caps the calcite formation process. From that point on, the inner exocuticle could be adjusted in its mineral content by active pore filament transport in connection with the underlying
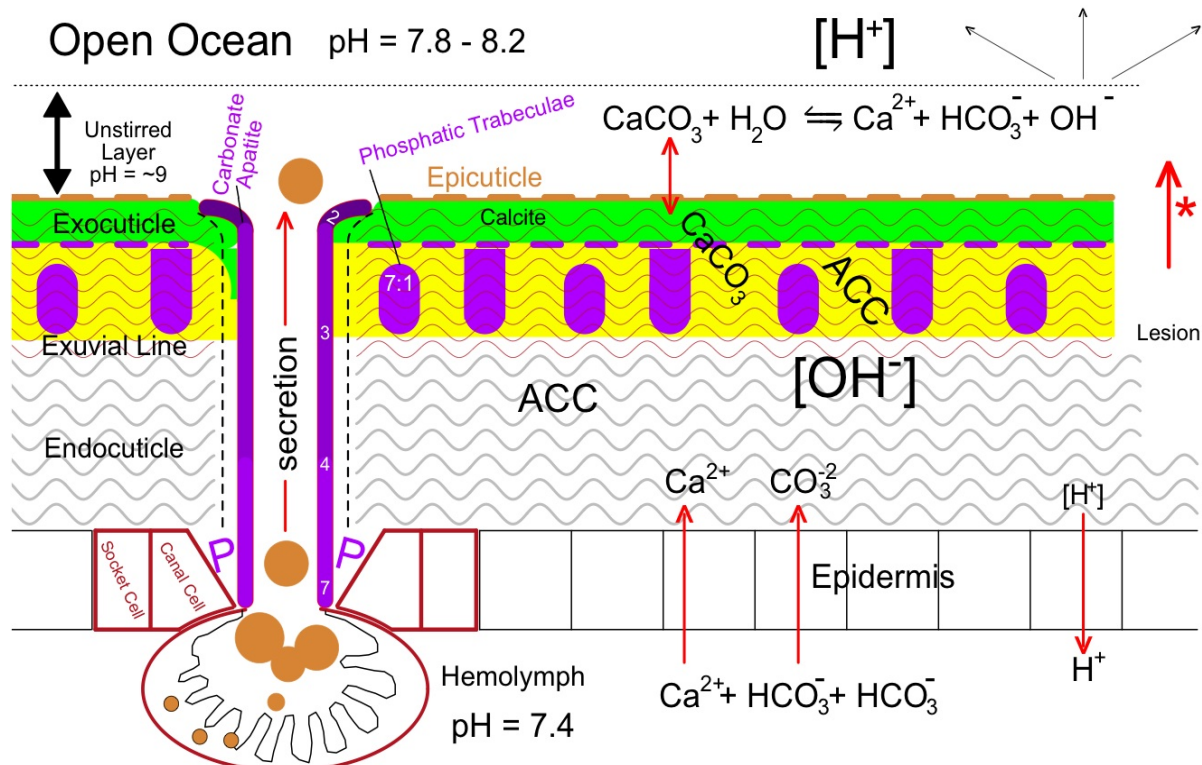
Figure 6. Structural model of lobster carapace cuticle illustrating the relationship of the structural uses of carbonate apatite and the cycle of calcium carbonate deposition and dissolution.

cells. The fourth type of phosphatic structure is seen as phosphate-rich cones of nascent cuticle projecting from the epidermal side of the membranous layer at locations where a canal will exit the interior of the cuticle. This is the location where new canal structure will be constructed during the intermoult period when new endocuticle is being added to the inner surface of the cuticle and the protective canals need to be extended inwardly. The Ca:P ratio of these cones is seen to be relatively low (3 in the three samples measured) and this ratio may represent the preparation of the membranous layer to produce canal structure.

A new mineral physiological model, Fig 6, was constructed with the benefit of the current EMP chemical analysis of the cuticle and measurements of the pH of the unstirred layer (Kunkel et al. 2012). This model suggests that an energy investment is needed to transport $CaCO_3$ from the $Ca(HCO_3)_2$ of the haemolymph to the membranous layer of the developing cuticle. This would most likely be achieved by transport of one bicarbonate with the counter transport of a proton across the epidermis. This would leave a basic cuticular space in which calcite could be formed and the remainder of the $CaCO_3$ remain amorphous depending upon the control of its crystallization by appropriate use of phosphate poisoning (Simkiss 1964).

On the environment-facing cuticle surface the dermal glands will have provided a secretion that provides mobile wax or greases that make the thin epicuticle layer semi-impermeable to dissolution of the cuticle. However, we have measured the pH and proton flux associated with normal cuticle and show that $CaCO_3$ is actively dissolving

into the unstirred layer adjacent to the epicuticle adjusting its pH toward the pKa of $CaCO_3$ which is pH 9 (Kunkel et al. 2012). When a lesion breaks through the epicuticle layer the full rate of dissolution of the calcite layer is brought to bear on the unstirred layer, making it yet more alkaline. Such alkalinity in the neighborhood of bacteria would certainly inhibit their rate of growth, motility and metabolism. Such inhibition is experienced by bacteria in general but not by eukaryotic microorganisms (Button 1985).

Our model of the cuticle based on the mapping of mineral content and measured ionic flux bears further examination and testing. A carbonate apatite trabecular infrastructure to the cuticle allows the presentation of our calcite immune response mechanism in the framework of an established arthropod cuticle structure. The trabeculae described here from calcium and phosphate maps of lobster cuticle can be seen to correspond to melanisation patterns seen in light microscope views of cuticle cross-sections of lobster cuticle (Kunkel et al. 2005).

The model is useful in that it provides numerous predictions that can be tested. For instance, the trabecular structure that is proposed to provide the rigidity of the intermoult cuticle would suggest that the distribution and development of the trabeculae would follow the widely used timetable used to test for development toward moulting by hardness of the chela, lateral carapace and dorsal carapace (Waddy et al. 1995). Environmental changes such as pH or phosphate availability might slow the availability of resources for the cuticle hardening process

and thus give microorganisms a longer time during which to initiate their attack on the lobster integument. Of particular interest would be testing of the model's proposed inhibitory effect of high pH in the unstirred layer on the growth, motility and development of a panel of normal surface living bacteria from the lobster integument. This model may also provide a heretofore under-appreciated general role for both calcite and carbonate apatite in other Crustaceans.

References

Al-Sawalmih A, Li C, Siegel S, Fratzl P, Paris O. 2009. On the stability of amorphous minerals in lobster cuticle. Advanced Materials 21:4011-15.

Buckeridge JS, Newman WA. 2006. A revision of the Iblidae and the stalked barnacles (Crustacea: Cirripedia: Thoracica), including new ordinal, familial and generic taxa, and two new species from New Zealand and Tasmanian waters. Zootaxa 1136:1-38.

Button DK. 1985. Kinetics of nutrient-limited transport and microbial growth. Microbiological Reviews 49:270-97.

Kühnel W. 2003. Color atlas of cytology, histology, and microscopic anatomy. Stuttgart: Thieme. 534 pages.

Kunkel JG, Jercinovic MJ, Callaham DA, Smolowitz R, Tlusty M. 2005. Electron microprobe measurement of mineralization of American lobster, *Homarus americanus*, cuticle: Proof of concept. 2005 Lobster Shell Disease Workshop, UMass Boston. New England Aquarium. Aquatic Forum Series, p 76-82.

Kunkel JG, Nagel W, Jercinovic MJ. 2012. Defense of the mineral fine structure of the American lobster cuticle. Journal of Shellfish Research. 31(2): 515-526.

Lawrence PA. 1966. Development and determination of hairs and bristles in the milkweed bug, *Oncopeltus fasciatus* (Lygaeidae, Hemiptera). Journal of Cell Science 1:475-98.

Lowenstam HA. 1981. Minerals formed by organisms. Science 211:1126-31.

Lowenstam HA, Weiner S. 1992. Phosphatic shell plate of the barnacle *Ibla* (Cirripedia): A bone-like structure. Proceedings of the National Academy of Sciences 89:10573#77.

Merritt DJ. 2007. The organule concept of insect sense organs: Sensory transduction and organule evolution. Advances in Insect Physiology 33:192-241.

Nikolov S, Petrov M, Lymperakis L, Friák M, Sachs C, Raabe D, et al. 2010. Revealing the design principles of high-performance biological composites using *ab initio* and multiscale simulations: the example of lobster cuticle. Advanced Materials 22:519-26.

Nikolov S, Fabritius H, Petrov M, Friá´k M, Lymperakis L, Sachs C, et al. 2011. Robustness and optimal use of design principles of arthropod exoskeletons studied by ab initio-based multiscale simulations. Journal of the Mechanical Behavior of Biomedical Materials 4:129-45.

Pe´rez W, Katz H, Lima M. 2008. Gross heart anatomy of Arctocephalus australis (Zimmerman, 1783). Anatomical Science International 83:6-10.

Pohl P, Saparov SM, Antonenko YN. 1998. The size of the unstirred layer as a function of the solute diffusion coefficient. Biophysical Journal 75:1403-09.

R Development Core Team. 2011. R: A language and environment for statistical computing. Vienna: R Foundation for Statistical Computing. Computer program. http://www.Rproject. org/ (accessed 16 October 2012).

Raabe D, Sachs C, Romano P. 2005. The crustacean exoskeleton as an example of a structurally and mechanically graded biological nanocomposite material. Acta Materialia 53:4281-92.

Romano P, Fabritius H, Raabe D. 2007. The exoskeleton of the lobster *Homarus americanus* as an example of a smart anisotropic biological material. Acta Biomater 3:301-09.

Simkiss K. 1964. Phosphates as crystal poisons. Biological Reviews 39:487#505.

Vega FJ, Da´vila-Alcocer VM, Filkorn HF 2005. Characterization of cuticle structure in Late Cretaceous and Early Tertiary decapod Crustacea from Mexico. Bull. Mizunami Fossil Museum 32:37-43.

Waddy SL, Aiken DE, deKleijn DPV. 1995. Control of growth and reproduction. In: Factor JR, editor. Biology of the Lobster *Homarus americanus*. New York,NY: Academic Press, p 217-66.